DOI: 10.61782/fa.2025.0330

EFFECTS OF INFLOW CONDITIONS ON TURBULENCE-INGESTION NOISE PREDICTION

Andrea Piccolo[1*] **Riccardo Zamponi**[1,2]
[1] Technische Universiteit Delft, Delft, The Netherlands
[2] von Karman Institute for Fluid Dynamics, Sint-Genesius-Rode, Belgium

ABSTRACT

In this paper, we present a modification of Amiet's model for rotating systems aimed at enhancing the assessment of inflow-conditions effects on turbulence-interaction noise generation and prediction. This involves replacing the original three-dimensional turbulence input, which is particularly challenging to measure both experimentally and numerically, with a one-dimensional term, enabling probe measurements to be directly used as input. The proposed modification also allows for the extension to rotating systems of turbulence-distortion models developed for rectilinear motion to account for realistic geometry effects in sound prediction. The approach is validated against experimental acoustic data obtained for a low-Reynolds two-bladed propeller interacting with grid-generated turbulence.

Keywords: *Rotating Systems, Turbulence Modeling, Turbulence-Ingestion Noise, Low-Fidelity Noise Prediction.*

1. INTRODUCTION

Aeroacoustic optimization of urban aerial vehicles is essential for the successful implementation of urban air mobility. Such a necessity arises from strict urban regulations and the complex, heterogeneous flow conditions that characterize urban environments. This highlights the importance of analyzing turbulence-ingestion noise (TIN), which results from the interaction between the incoming turbulence structures and the rotor. The complexity is further increased by the growing diversity of rotor geometries and configurations, making flow-structure interactions even more challenging to predict and control.

The interaction of turbulence with a rotating system can be divided into three distinct phases. In the first phase, the streamtube contraction induced by the rotating system elongates the turbulence structures in the streamwise direction [1]. Consequently, even if the incoming turbulence is homogeneous and isotropic far upstream, the rotor encounters anisotropic flow conditions [1, 2]. In the second phase, these elongated structures are chopped by the rotor blades, generating coherent unsteady surface pressure across different blades. This blade-to-blade correlation introduces narrow-band quasi-tonal peaks to the mainly broadband features of the TIN spectra. Finally, in the third phase, the elongated and chopped structures undergo distortion as they interact with the blade leading edge, accelerating along its surface. Although the impact of this mechanism on noise generation has been extensively studied in the context of rectilinear motion [3, 4], its potential effects on rotating systems remain largely unexplored.

Since the identification of this flow-induced noise source by Sharland in the 1960s [5], several low-fidelity models — mainly used for the optimization phase — have been developed, with Amiet's model [6] standing out for its robustness and simplicity. Despite its numerous simplifying assumptions, this model has proven capable of providing accurate predictions across a wide range of conditions [7]. It also accounts for blade-to-blade correlation and partially incorporates rotor geometry by discretizing the blade into narrow strips using a strip-theory approach [8]. However, its implementation depends on precise modeling or extensive characterization of inflow conditions, which poses a significant limitation for many

*__*Corresponding author*__: *a.piccolo@tudelft.nl.*

cutting-edge configurations currently under development.

The purpose of this study is hence to propose a modification to Amiet's model that enables the use of direct, simple flow measurements as input. This modification is especially useful for complex configurations where low-fidelity noise prediction is needed but a detailed description or reliable model of the inflow is unavailable, allowing the use of hot-wire anemometry measurements to assess the acoustic performances. The modified model has been validated against experimental measurements from a simple turbulence-rotor configuration.

The outline of the paper is the following. The experimental setup is presented in Sec. 2, while the modification and the results are reported in Sec. 3. The conclusions are then drawn in Sec. 4.

2. METHODOLOGY

The experimental campaign has been carried out in the anechoic open-jet wind tunnel (A-Tunnel) at the Low-Speed Laboratory of TU Delft, shown in Fig. 1a and extensively described by Merino-Martinez *et al.* [9]. A turbulence-generating grid (with rectangular rods $0.01\,\mathrm{m}$ wide separated by $0.10\,\mathrm{m}$) has been placed at the exit of the tunnel, followed by a $0.60\,\mathrm{m}$ long circular nozzle with a diameter of $0.60\,\mathrm{m}$. This configuration was chosen to prevent microphone measurements from being contaminated with grid noise.

The propeller is an APC 9×6 rescaled to have a diameter of $0.30\,\mathrm{m}$ and modified to feature a NACA 4412 as blade section. Positioned $0.40\,\mathrm{m}$ from the nozzle exit, the propeller is powered by a Lehner Motors LMT 2280/34 brushless inrunner. Further information about the propeller manufacturing and the support nacelle is provided by Grande *et al.* [10]. A single rotational speed of $6000\,\mathrm{RPM}$ has been considered, resulting in an advance ratio $J = W_\infty/nD$, with n being the rotational speed in Hz, of 0.30.

Figure 1b shows a schematic of the experimental setup. The reference frame is centered on the rotor hub, with the z axis aligned along the axial (streamwise) direction, pointing upstream. The x and y axes lie within the rotor plane, forming a right-handed coordinate system. The corresponding velocity components are denoted as w, u, and v.

The sketch also illustrates the placement of ten G.R.A.S. 40PH microphones along the directivity arc at a radius of $R_{\text{mic}} = 1.3\,\mathrm{m}$, positioned between $\theta_{\text{mic}} = 60°$ and $\theta_{\text{mic}} = 150°$ in increments of $10°$, with θ_{mic} measured relative to the z axis. The microphones have a frequency range of 10 to $20\,\mathrm{kHz}$ and a maximum sound pressure level of $135\,\mathrm{dB}$.

Aerodynamic measurements were conducted using hot-wire anemometry (HWA). Axial velocity fluctuations were recorded at the grid points shown in Fig. 1b. The probe used is a platinum-plated tungsten Dantec Dynamics P11, with a width of $5\,\mu\mathrm{m}$ and a length of $1.25\,\mathrm{mm}$. HWA data were used to characterize the flow at the nozzle exit, where the free-stream velocity is $W_\infty = 9.5\,\mathrm{m\,s^{-1}}$, the turbulence intensity $\sqrt{\overline{w'^2}}$ is $6\,\%$, and the integral length scale L^z_{ww} is $0.018\,\mathrm{m}$.

Acoustic and aerodynamic data were collected for $60\,\mathrm{sec}$ at a sampling rate of $51.2\,\mathrm{kHz}$. The power spectral densities (PSDs) were computed using Welch's method with a Hanning window and a $50\,\%$ overlap, achieving a frequency resolution of $1\,\mathrm{Hz}$.

3. RESULTS

Amiet's model for turbulence-ingestion noise prediction [6] is based on the analytical approach developed in the two-dimensional regime [11]. This is used to calculate the instantaneous sound emission of the blade at each azimuthal position γ, which is hence modeled as if the blade were moving in rectilinear motion. This assumption holds as long as the considered noise frequencies are much higher than the rotational frequency of the propeller.

From a modeling perspective, the implementation of the rectilinear motion model requires three key considerations. First, an average must be taken over the azimuth. Second, the relative motion of the source with respect to the listener's position must be taken into account, which means that the listener's position $\mathbf{x}_\mathrm{B} = (x_\mathrm{B}, y_\mathrm{B}, z_\mathrm{B})$ should be calculated in the reference frame moving with the blade (from which the subscript $_\mathrm{B}$). Third, the Doppler effect must be incorporated into the calculation. The following equation is then finally retrieved for the far-field acoustic pressure $S_{pp}(\mathbf{x}_\mathrm{B}, \omega_0)$

$$S_{pp}(\mathbf{x}_\mathrm{B}, \omega_0) = \frac{1}{2\pi}\int_0^{2\pi}\left(\frac{\omega_\mathrm{B}}{\omega_0}\right)^2 S_{pp}(\mathbf{x}_\mathrm{B}, \omega_\mathrm{B}, \gamma)\,\mathrm{d}\gamma, \tag{1}$$

with $\omega_\mathrm{B}/\omega_0$ indicating the Doppler's effect as the ratio between ω_B, i.e., the "de-Dopplerized" frequency in the rotating reference frame, and ω_0, i.e., the "Dopplerized" sound frequency as heard by the observer in the fixed reference frame.

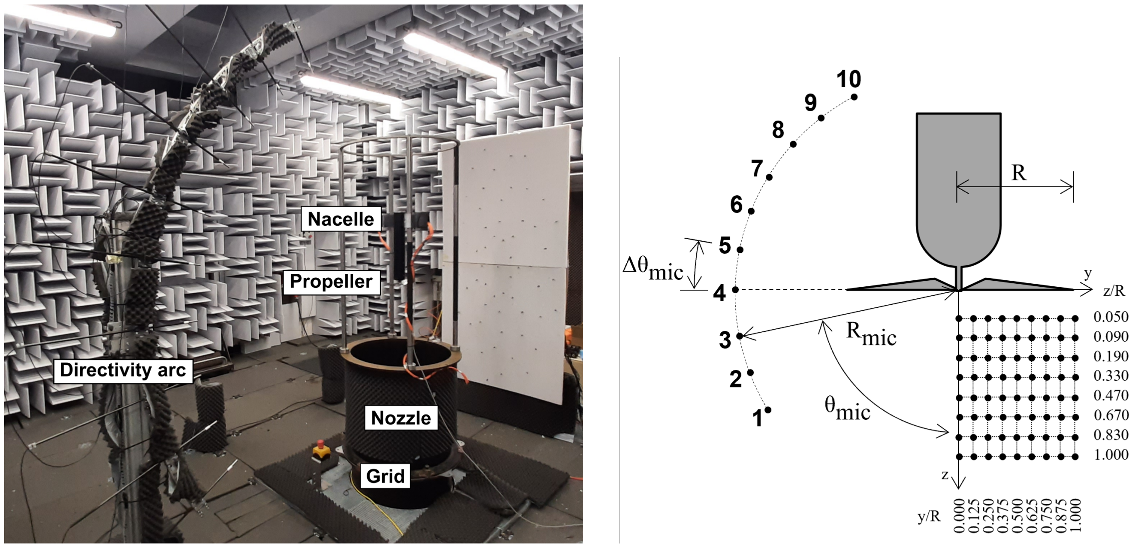

(a) (b)

Figure 1: (a) Picture and (b) sketch of the experimental setup at the TU Delft A-tunnel facility.

In the formulation incorporating blade-to-blade correlation, the instantaneous noise emission generated by the blade in the rotating reference system $S_{pp}\left(\mathbf{x}_{\mathrm{B}}, \omega_{\mathrm{B}}, \gamma\right)$ is expressed as

$$S_{pp}\left(\mathbf{x}_{\mathrm{B}}, \omega_{\mathrm{B}}, \gamma\right) = \left(\frac{\omega_{\mathrm{B}} z_{\mathrm{B}} \rho_0 c}{2 c_0 \sigma^2}\right)^2 \pi U_{\mathrm{x}} \left(\frac{L}{2}\right) \times \overline{w'^2} \left(\frac{c}{2}\right)^2 \left|\mathcal{L}\left(K_x, K_y, M_x\right)\right|^2 \times \sum_{n=-\infty}^{\infty} \Phi_{ww}\left(K_x, K_y, K_z^{(n)}\right) \frac{2\pi}{\left(\frac{c}{2}\right)^2 \overline{w'^2} Z}, \quad (2)$$

with ρ_0 being the flow density, c_0 is the speed of sound, c the chord and L the span, while $\sigma_0 = \sqrt{x_{\mathrm{B}}^2 + \beta_x^2 \left(y_{\mathrm{B}}^2 + z_{\mathrm{B}}^2\right)}$, with $\beta_x = \sqrt{1 - M_x^2}$, considers convection effects. U_x, with the respective Mach number M_x, indicates the flow velocity along the blade chord that accounts for the local pitch angle, as in the approach of Sinayoko *et al.* [12]. $\mathcal{L}\left(K_x, K_y, M_x\right)$ is the aeroacoustic transfer function, for which the original formulation of Amiet [13] has been implemented, and $\Phi_{ww}\left(K_x, K_y, K_z^{(n)}\right)$ is the three-dimensional turbulence spectrum. The wavenumbers are obtained as $K_x = \frac{\omega_{\mathrm{B}}}{U_{\mathrm{x}}}$, $K_y = \frac{\omega_{\mathrm{B}} y_{\mathrm{B}}}{c_0 \sigma}$, and $K_z^{(n)} = \frac{2\pi n + \omega_0 T_2}{Z}$. The expression for $K_z^{(n)}$ is obtained in the framework of the blade-to-blade correlation: T_2 is the time between the eddie chops as heard by the listener, Z can be defined as the distance between the blade paths in fluid, and n is an index representing the correlation between the 0-th and the n-th blade. As a detailed overview of the model falls outside the scope of the present manuscript, the reader is referred to Amiet [6, 13] for the derivation and expressions of all the parameters.

The present implementation considers the inverse strip theory approach proposed by Christope *et al.* [8] to calculate the blade noise emission. With this methodology, the blade is divided into M narrow-span strips of width L/M, whose emitted sound is calculated as the difference between a wing of span L_1 and a wing of span $L_2 = L_1 - L/M$, with $L_1, L_2 >> 1$. Referring to Eq. 2, this hence leads for $S_{pp}\left(\mathbf{x}_{\mathrm{B}}, \omega_{\mathrm{B}}, \gamma\right)$ for the m-th strip to

$$S_{pp}\left(\mathbf{x}_{\mathrm{B}}, \omega_0, \gamma\right)\Big|_m = \left(S_{pp}\left(\mathbf{x}_{\mathrm{B}}, \omega_0, \gamma\right)\Big|_{L_1} + - S_{pp}\left(\mathbf{x}_{\mathrm{B}}, \omega_0, \gamma\right)\Big|_{L_2}\right)\Big|_m. \quad (3)$$

Finally, Eq. 1 must be applied for all the M strips and the B blades, yielding

$$S_{pp}\left(\mathbf{x}_{\mathrm{B}}, \omega_0\right) = B \sum_{m=1}^{M} S_{pp}\left(\mathbf{x}_{\mathrm{B}}, \omega_0\right)\Big|_m. \quad (4)$$

The present study proposes the substitution of the three-dimensional turbulence spectrum $\Phi_{ww}\left(K_x, K_y, K_z^{(n)}\right)$ in Eq. 2 with a one-dimensional one $\Theta_{ww}\left(K_x\right)$ to allow the use of direct probe measurements. This is carried out using the analytical results of Wilson [14] on the multi-dimensional correlation and wavenumber spectra of homogeneous isotropic turbulence. The findings indeed show that it is possible to write

$$\Phi_{ww}\left(K_x, K_y, K_z^{(n)}\right) = \Psi_{ww}\left(K_x, K_y\right) \times \tilde{A}\left(K_x, K_y, K_z^{(n)}\right), \quad (5)$$

with $\tilde{A}\left(K_x, K_y, K_z^{(n)}\right)$ indicating an auxiliary function and $\Psi_{ww}\left(K_x, K_y\right)$ being the two-dimensional wavenumber spectrum. $\tilde{A}\left(K_x, K_y, K_z^{(n)}\right)$ can be calculated by performing the ratio of the von Kármán analytical expression of $\Phi_{ww}\left(K_x, K_y, K_z^{(n)}\right)$ and $\Psi_{ww}\left(K_x, K_y\right)$ [15], obtaining

$$\tilde{A}\left(K_x, K_y, K_z^{(n)}\right) = \left(\frac{55}{16}\frac{L_{ww}^z}{\pi}\right) \times \frac{\left(1+\left(\frac{K_x}{k_e}\right)^2+\left(\frac{K_y}{k_e}\right)^2\right)^{\frac{7}{3}}}{\left(1+\left(\frac{K_x}{k_e}\right)^2+\left(\frac{K_y}{k_e}\right)^2+\left(\frac{K_z^{(n)}}{k_e}\right)^2\right)^{\frac{17}{6}}}, \quad (6)$$

with $k_e = \pi / L_{ww}^z \Gamma\left(5/6\right) / \Gamma\left(1/3\right)$.

The two-dimensional wavenumber spectrum is then converted into a one-dimensional spectrum following the formulation of Amiet [11]

$$\Psi_{ww}\left(K_x, K_y\right) = \frac{1}{\pi}\Theta_{ww}\left(K_x\right) l_y\left(K_x\right), \quad (7)$$

with l_y being the spanwise coherence length of the upwash velocity component, for which the following expression is derived:

$$l_y\left(K_x\right) = \frac{8L_{ww}^z}{3}\left[\frac{\Gamma\left(1/3\right)}{\Gamma\left(5/6\right)}\right]^2 \times \frac{\left(\frac{K_x}{k_e}\right)^2}{\left(3+8\left(\frac{K_x}{k_e}\right)^2\right)\sqrt{1+\left(\frac{K_x}{k_e}\right)^2}}. \quad (8)$$

The introduction of the two auxiliary functions $\tilde{A}\left(K_x, K_y, K_z^{(n)}\right)$ and $l_y\left(K_x\right)$ thus allows the turbulence term in Eq. 2 to be expressed in terms of the one-dimensional spectrum, finally leading to

$$S_{pp}\left(\mathbf{x}_\mathrm{B}, \omega_\mathrm{B}, \gamma\right) = \left(\frac{\omega_\mathrm{B} z_\mathrm{B} \rho_0 c}{2 c_0 \sigma^2}\right)^2 \pi U_\mathrm{x}\left(\frac{L}{2}\right) \times \overline{w'^2}\left(\frac{c}{2}\right)^2 \left|\mathcal{L}\left(K_x, K_y, M\right)\right|^2 \left(\frac{1}{\pi}\Theta_{ww}\left(K_x\right) l_y\left(K_x\right)\right) \times \sum_{n=-\infty}^{\infty} \tilde{A}\left(K_x, K_y, K_z^{(n)}\right) \frac{2\pi}{\left(\frac{c}{2}\right)^2 \overline{w'^2} Z}. \quad (9)$$

The inclusion of a one-dimensional turbulence term enables the application of the altered spectra provided by turbulence-distortion models [3, 16]. Originally developed for bidimensional regime, these approaches effectively characterize the impact of thick airfoil geometries on noise generation.

Alternatively, the one-dimensional spectrum can be obtained using a direct probe measurement in the frequency domain as input, such as the frequency spectra of axial velocity - corresponding to the upwash component with respect to the propeller - obtained by means of HWA in the rotor inflow. These are shown in Fig. 2, which compares the measurements taken far upstream at $z/\mathrm{R} = 1.000$, at an intermediate distance $z/\mathrm{R} = 0.470$, and in the vicinity of the propeller at $z/\mathrm{R} = 0.050$ for 4 radial positions ($y/\mathrm{R} = 0.125$, $y/\mathrm{R} = 0.375$, $y/\mathrm{R} = 0.625$, and $y/\mathrm{R} = 0.875$). A decrease in velocity fluctuations in the low-frequency range, up to $f/\mathrm{BPF} \simeq 0.7$, can be observed as the frequency spectrum of the axial velocity is sampled closer to the rotor plane, especially for the mid-radial positions. This results from the alteration of turbulent structures as they are elongated in the streamtube contraction induced by the propeller, as in the case of the converging section of a wind tunnel [17, 18].

Such a mechanism also impacts sound production, as can be inferred by applying Amiet's model with the HWA spectra as input using Eq. 9. A filtering operation was applied to the velocity spectra sampled at intermediate distances and very close to the rotor plane to remove the tones caused by the blade passage. The resulting noise prediction is shown in Fig. 3, which shows the sound pressure level (SPL) at microphone positions 1 and 8. A clear variation in noise levels is observed in the low-frequency range when the sampling position of the velocity spectrum

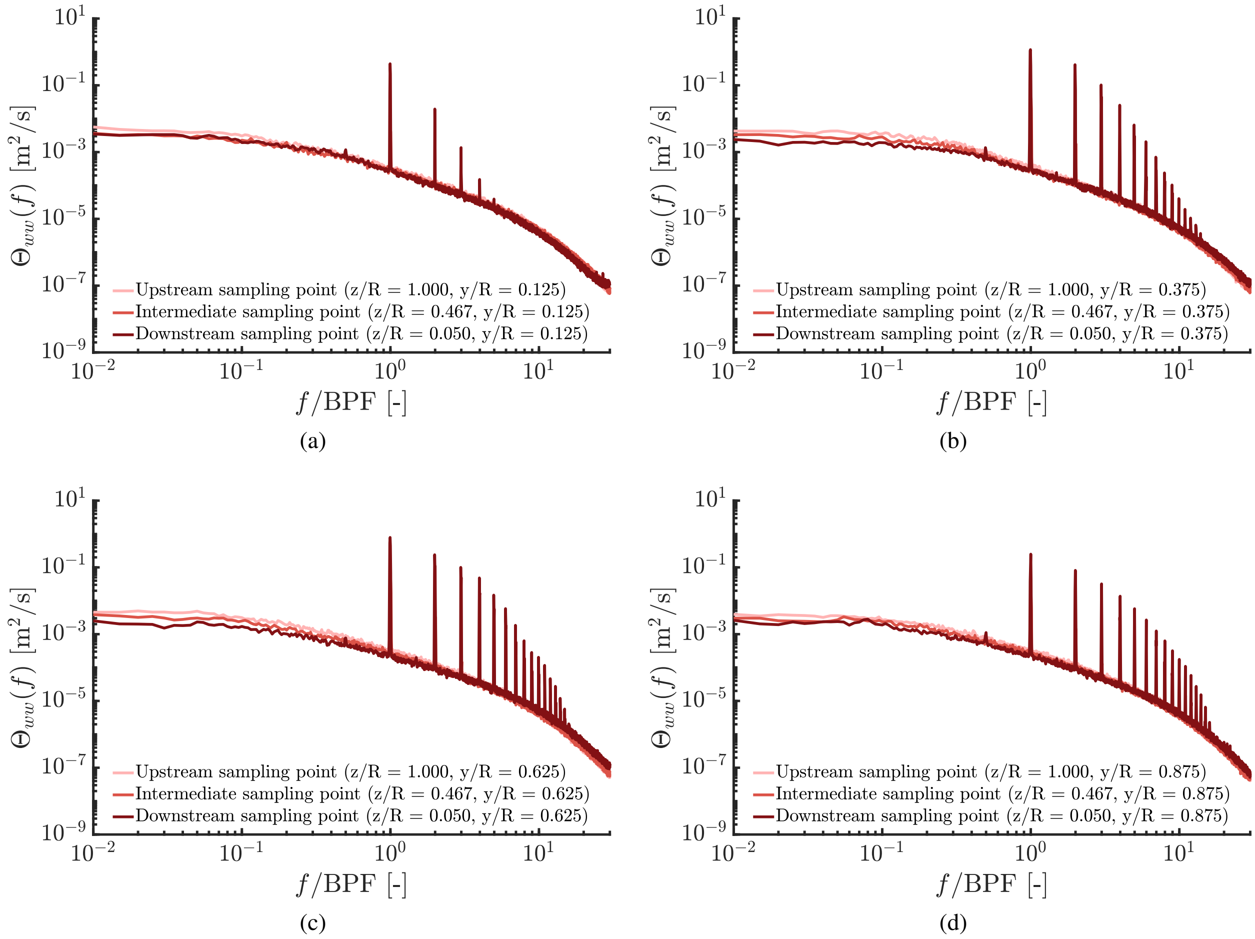

Figure 2: Frequency spectra of the axial velocity at radial positions (a) $y/\mathrm{R} = 0.125$, (b) $y/\mathrm{R} = 0.375$, (c) $y/\mathrm{R} = 0.625$, and (d) $y/\mathrm{R} = 0.875$. The spectra sampled far upstream at $z/\mathrm{R} = 1.000$, at intermediate distance $z/\mathrm{R} = 0.470$, and in the vicinity of the propeller at $z/\mathrm{R} = 0.050$ are compared.

is changed, with higher accuracy achieved by sampling closer to the rotor plane.

4. CONCLUSIONS

An implementation of Amiet's model for turbulence-ingestion noise in rotating systems has been proposed to allow direct flow measurements obtained through hot-wire anemometry to be used as input. This modification was validated using experimental data from a two-bladed propeller interacting with grid-generated turbulence. It was found that the variation in the inflow characteristics as the rotor plane is approached significantly affects the noise generation and prediction. This effect was evaluated by changing the position at which the HWA velocity spectrum, used as input for the model, is sampled. The results confirm that this modification of Amiet's model can effectively assess the impact of inflow conditions and play a crucial role in providing low-fidelity predictions of acoustic performance for configurations with limited availability of flow measurements and modeling.

5. REFERENCES

[1] D. B. Hanson, "Spectrum of rotor noise caused by atmospheric turbulence," *The Journal of the Acoustical Society of America*, vol. 55, pp. S3–S4, Apr. 1974.

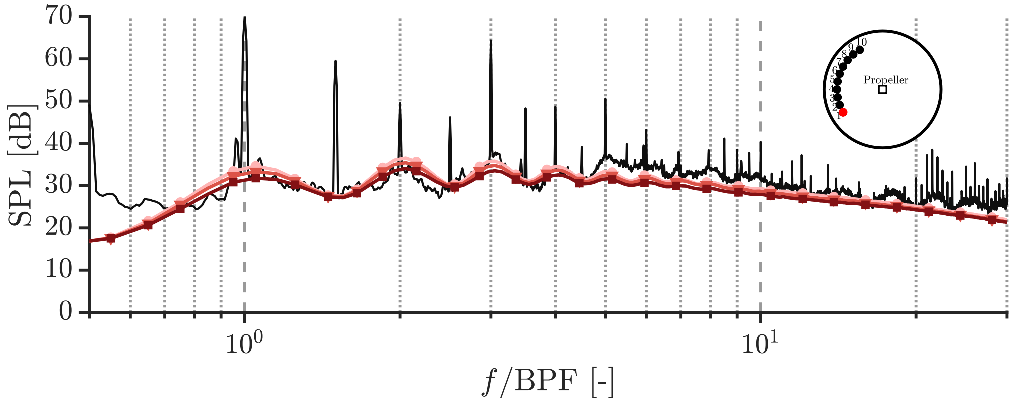

(a)

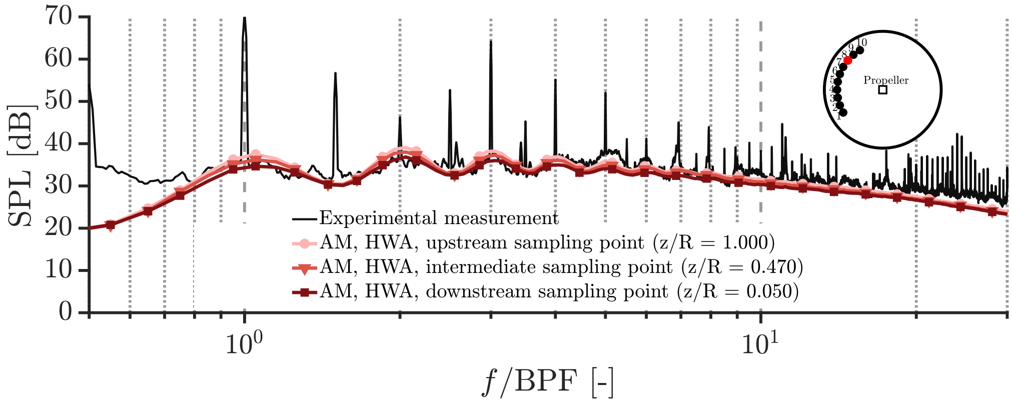

(b)

Figure 3: Sound pressure level calculated with Amiet's model (AM) applied using HWA spectra sampled far upstream ($z/\mathrm{R} = 1.000$), at an intermediate distance ($z/\mathrm{R} = 0.470$), and in the vicinity of the propeller ($z/\mathrm{R} = 0.050$) compared to experimental measurements for (a) Microphone 1 and (b) Microphone 8. The reference pressure used to calculate the SPL is 2×10^{-5} Pa.

[2] S. J. Majumdar and N. Peake, "Noise generation by the interaction between ingested turbulence and a rotating fan," *J. Fluid Mech.*, vol. 359, pp. 181–216, Mar. 1998.

[3] F. L. dos Santos, L. Botero-Bolívar, C. Venner, and L. De Santana, "Modeling the Turbulence Spectrum Dissipation Range for Leading-Edge Noise Prediction," *AIAA Journal*, pp. 1–12, Mar. 2022.

[4] A. Piccolo, R. Zamponi, F. Avallone, and D. Ragni, "Turbulence distortion and leading-edge noise," *Physics of Fluids*, 2024.

[5] I. J. Sharland, "Sources of noise in axial flow fans," *Journal of Sound and Vibration*, vol. 1, pp. 302–322, July 1964.

[6] R. Amiet, "Noise produced by turbulent flow into a propeller or helicopter rotor," in *3rd Aeroacoustics Conference*, Aeroacoustics Conferences, American Institute of Aeronautics and Astronautics, July 1976.

[7] H. Raposo and M. Azarpeyvand, "Turbulence ingestion noise generation in rotating blades," *Journal of Fluid Mechanics*, vol. 980, p. A53, Feb. 2024.

[8] J. Christophe, J. Anthoine, and S. Moreau, "Amiet's

Theory in Spanwise-Varying Flow Conditions," *AIAA Journal*, vol. 47, pp. 788–790, Mar. 2009.

[9] R. Merino-Martínez, A. Rubio Carpio, L. T. Lima Pereira, S. Van Herk, F. Avallone, D. Ragni, and M. Kotsonis, "Aeroacoustic design and characterization of the 3D-printed, open-jet, anechoic wind tunnel of Delft University of Technology," *Applied Acoustics*, vol. 170, p. 107504, Dec. 2020.

[10] E. Grande, G. Romani, D. Ragni, F. Avallone, and D. Casalino, "Aeroacoustic Investigation of a Propeller Operating at Low Reynolds Numbers," *AIAA Journal*, vol. 60, pp. 860–871, Feb. 2022.

[11] R. K. Amiet, "Acoustic radiation from an airfoil in a turbulent stream," *Journal of Sound and Vibration*, vol. 41, pp. 407–420, Aug. 1975.

[12] S. Sinayoko, M. Kingan, and A. Agarwal, "Trailing-edge noise theory for rotating blades in uniform flow," 2013.

[13] R. K. Amiet, "Noise Produced by Turbulent Flow into a Rotor: Theory Manual for Noise Calculation," NASA Report, 1989.

[14] D. K. Wilson, "Three-Dimensional Correlation and Spectral Functions for Turbulent Velocities in Homogeneous and Surface-Blocked Boundary Layers.:," tech. rep., Defense Technical Information Center, Fort Belvoir, VA, July 1997.

[15] S. Glegg and W. Devenport, "Chapter 9 - Turbulent flows," in *Aeroacoustics of Low Mach Number Flows* (S. Glegg and W. Devenport, eds.), pp. 185–220, Academic Press, Jan. 2017.

[16] D. De Santana, J. Christophe, C. Schram, and W. Desmet, "A Rapid Distortion Theory modified turbulence spectra for semi-analytical airfoil noise prediction," *Journal of Sound and Vibration*, vol. 383, pp. 349–363, Nov. 2016.

[17] R. K. Amiet, J. C. Simonich, and R. H. Schlinker, "Rotor noise due to atmospheric turbulence ingestion. II - Aeroacoustic results," *Journal of Aircraft*, vol. 27, pp. 15–22, Jan. 1990.

[18] G. K. Batchelor and I. Proudman, "The Effect of Rapid Distortion of a Fluid in Turbulent Motion," *The Quarterly Journal of Mechanics and Applied Mathematics*, vol. 7, pp. 83–103, Jan. 1954.